Perpendicular diffusion of a dilute beam of charged dust particles in a strongly coupled dusty plasma

Bin Liu and J. Goree
Department of Physics and Astronomy, The University of Iowa, Iowa City, Iowa 52242, USA

(Received 13 May 2014; accepted 11 June 2014; published online 27 June 2014)

The diffusion of projectiles drifting through a target of strongly coupled dusty plasma is investigated in a simulation. A projectile's drift is driven by a constant force **F**. We characterize the random walk of the projectiles in the direction perpendicular to their drift. The perpendicular diffusion coefficient $D_{p\perp}$ is obtained from the simulation data. The force dependence of $D_{p\perp}$ is found to be a power law in a high force regime, but a constant at low forces. A mean kinetic energy W_p for perpendicular motion is also obtained. The diffusion coefficient is found to increase with W_p with a linear trend at higher energies, but an exponential trend at lower energies. © *2014 AIP Publishing LLC*. [http://dx.doi.org/10.1063/1.4885353]

I. INTRODUCTION

We investigate the diffusion of a dilute beam of charged projectiles as they scatter on particles in a strongly coupled dusty plasma. A dusty plasma contains small solid particles, which we call dust particles. They become highly charged by collecting more electrons than ions.[1–13] Laboratory dusty plasmas also have a significant quantity of neutral gas. Due to the large charge, a collection of dust particles can be strongly coupled, with more potential energy than thermal kinetic energy, so that the collection of dust particles self-organizes with a liquid-like or solid-like microscopic structure.[14] Such a strongly coupled dusty plasma can fill a three-dimensional (3D) volume in microgravity experiments.[15–19]

Self-diffusion, which is a random walk of individual particles, has been studied in dusty plasmas experimentally[20–31] and numerically.[32–53] In the previous numerical studies, diffusion was characterized under equilibrium conditions. Here, we investigate diffusion under a nonequilibrium condition: in particular, we consider the random walk of a projectile beam that drifts through a dusty plasma due to a constant force. An additional difference, as compared to the previous numerical papers, is that the random walk here is not a self-diffusion: the projectile diffusion occurs mainly due to collisions with target particles that have a different size.

The drift of the projectiles with respect to the target particles is driven by a net force **F**, which can arise in a dusty plasma due to an imbalance of forces such as the electric and ion drag forces. Those forces scale differently with particle size,[54] so that in a mixture of two particle sizes, one size of particles can be forced to drift through particles of another size. The target particles may be stationary, or drifting. In some previous microgravity experiments, target particles were stationary while large quantities of smaller projectiles drifted through the targets.[55–57]

We simulate a case similar to those experiments, except that we consider smaller quantities of projectiles, so that they interact only with targets, but rarely with other projectiles. For such a dilute beam of projectiles, we previously[58] characterized the drifting motion parallel to **F** to find the drift velocity u_p. We determined the mobility $\mu_p = u_p/F$, which is a constant for low F, but an increasing function of F at high F. Here, we investigate another transport coefficient, the diffusion coefficient, to characterize motion of the projectiles.

In addition to the parallel drift, the projectiles will also be scattered randomly in the direction perpendicular to **F**. This random perpendicular scattering occurs due to collisions of the projectiles mainly with target particles, and to a lesser extent with gas atoms. The result is a diffusion of the projectiles in the direction perpendicular to **F**, which we characterize here. The main result of this paper is a quantification of this diffusion coefficient, $D_{p\perp}$. We also determine the kinetic energy W_p for perpendicular motion in the dilute beam. We find the scaling laws of $D_{p\perp}$ for varying values of F and W_p.

II. SIMULATION

Using a molecular-dynamics approach, we integrate the Langevin equations

$$m_t\ddot{\mathbf{x}}_i = -\nu_t m_t\dot{\mathbf{x}}_i + \zeta_{ti}(t) - \sum_k \nabla\phi_{ik} - \nabla\Phi, \quad (1)$$

$$m_p\ddot{\mathbf{x}}_j = -\nu_p m_p\dot{\mathbf{x}}_j + \zeta_{pj}(t) - \sum_k \nabla\phi_{jk} - \nabla\Phi + \mathbf{F}. \quad (2)$$

Equation (1) is for the target particles of mass m_t, as denoted by the subscript t, while Eq. (2) is for the projectiles of mass m_p. Processes taken into account include dust-gas collisions, the dust-dust interaction $-\nabla\phi$, the electric force due to a confining potential $-\nabla\Phi$, and a constant force **F** that is applied to projectiles only as in Ref. 58. Dust-gas collisions are represented by two terms: a fluctuating force ζ and a frictional drag term. The drag term has a friction coefficient, ν_p or ν_t, for projectile or target particles, respectively. Differently from most Langevin simulations, we augment ζ above that predicted by the

fluctuation-dissipation theorem in order to account for additional heating mechanisms that may be present, in addition to collisions with gas atoms.[59]

The dust-dust interaction for a particle pair i and j, with charges Q_i and Q_j, is described by the Yukawa potential

$$\phi(r_{ij}) = \frac{Q_i Q_j}{4\pi\epsilon_0}\frac{e^{-r_{ij}/\lambda_D}}{r_{ij}}, \tag{3}$$

where λ_D is a screening length and r_{ij} is the separation. A collection of particles interacting with this potential can be characterized by two dimensionless parameters: the screening parameter κ and the Coulomb coupling parameter Γ_t. The screening parameter is

$$\kappa = a/\lambda_D, \tag{4}$$

where a is a typical interparticle distance. The Coulomb coupling parameter for the target particles is

$$\Gamma_t = Q_t^2/4\pi\epsilon_0 a k_B T_t, \tag{5}$$

where Q_t and $k_B T_t$ are the charge and the kinetic energy of target particles, respectively. In Eqs. (4) and (5), we characterize the typical interparticle distance a as the Wigner-Seitz radius $a = (3/4\pi n_t)^{1/3}$, where n_t is the number density of the target particles. Choosing some other convention for the interparticle distance would cause κ and Γ_t to have systematically larger or smaller values.

The 3D system we simulate consists of $N = 12\,800$ or $57\,600$ target particles, along with a small number of projectiles. The target particles are not drifting. Due to the confinement force $-\nabla\Phi$, the target particles are limited to a rectangular volume, with a number density of $n_t = 3 \times 10^4\,\mathrm{cm}^{-3}$ and a corresponding interparticle distance of $a = 0.02\,\mathrm{cm}$.

We use finite boundary conditions, with a confining potential that is flat in most of the volume, and a rising parabola at the edge. The confining potential is

$$\Phi = \psi(x,b) + \psi(y,c) + \psi(z,d), \tag{6}$$

where

$$\psi(x,b) = \begin{cases} 0, & |x| < b \\ m_t\omega_e^2(|x| - b)^2/2, & |x| \geq b, \end{cases} \tag{7}$$

and similarly for y and z. The constants b, c, and d are the half widths of our simulation box along the x, y, and z axes, respectively. For our simulation with $N = 12\,800$, these constants are $b = 66.0\lambda_D$, $c = 40.5\lambda_D$, and $d = 34.7\lambda_D$. For the larger simulation with $N = 57\,600$, they are $b = 131.5\lambda_D$, $c = 61.0\lambda_D$, and $d = 52.0\lambda_D$. The constant ω_e, which is chosen to be $\sqrt{Q_t^2/4\pi\epsilon_0 m_t \lambda_D^3}$, characterizes the parabolic confinement at the edge.

A projectile is introduced on the smallest face of the rectangular volume, and it is then driven by the force $\mathbf{F}$ (which has a direction parallel to the longest face) to move through the volume. At first, there is an initial transient due to the acceleration of the projectile in the parabolic edge; we do not analyze this early portion of the trajectories. After a short time, the projectile drifts with an average speed u_p, and this is the portion of the trajectories that we analyze. Further details of the simulation are in Ref. 58.

The constant force $\mathbf{F} = F\hat{x}$ is applied only to projectiles. The perpendicular diffusion that we studied here involves the random motion in the $\hat{y}$ and $\hat{z}$ directions.

Here, we list key parameters in our simulation. We choose a smaller particle radius of $0.64\,\mu\mathrm{m}$ ($m_p = 1.66 \times 10^{-15}\,\mathrm{kg}$) for the projectiles, but a larger radius of $3.43\,\mu\mathrm{m}$ ($m_t = 2.55 \times 10^{-13}\,\mathrm{kg}$) for the target particles. For neon at 50 Pa pressure and 0.03 eV temperature, the gas friction coefficients[11,60] are: $\nu_p = 273\,\mathrm{s}^{-1}$ and $\nu_t = 51\,\mathrm{s}^{-1}$. The particle charges are $Q_p = -1590e$ for the projectiles, and $Q_t = -8520e$ for the target particles. In a strongly coupled plasma, the time scale for collisions is comparable to the inverse plasma frequency ω_t^{-1}, where

$$\omega_t = \sqrt{Q_t^2 n_t/\epsilon_0 m_t}. \tag{8}$$

For our simulated parameters, $\omega_t = 157\,\mathrm{s}^{-1}$. The Debye length is $\lambda_D = 8.3 \times 10^{-3}\,\mathrm{cm}$. These parameters are generally consistent with those in the PK-4 instrument.[57,61,62]

The target conditions we simulate are typical of a liquid state. The screening parameter is $\kappa = 2.4$, for $a = 0.02\,\mathrm{cm}$. Liquids at two temperatures are simulated: a hot liquid at $T_t = 10T_m$ and a cold liquid at $T_t = 2T_m$. The corresponding coupling parameters are $\Gamma_t = 62$ and 310, respectively. Here, T_m is the melting point[63] for the 3D Yukawa system of target particles.

Our results are presented in dimensionless units. The distance, time, velocity, force, energy, and diffusion coefficient are normalized by a, ω_t^{-1}, $a\omega_t$, $m_p\omega_t^2 a$, $m_t(\omega_t a)^2/3$, and $a^2\omega_t$, respectively.

The projectile's motion was found in Ref. 58 to have at least two force regimes. The low and high regimes correspond to near-equilibrium and nonequilibrium conditions, respectively. In the low regime, the mobility μ_p for the parallel drift motion remains constant, while it is not a constant and increases with F in the high regime. The transition between two regimes, which is best distinguished by a change in the trend for the perpendicular projectile velocity, occurs at $F \approx 2$ or $3\,m_p\omega_t^2 a$, for $T_t = 2T_m$ or $10T_m$, respectively. In addition to the two regimes discussed above, a third regime, due to a dominant role of gas friction, was also speculated to exist at even higher forces.[58]

We determine the diffusion coefficient $D_{p\perp}$ using projectile displacements to calculate a probability distribution function (PDF). For a given starting time, we calculate the displacement in the $\hat{y}$ and $\hat{z}$ directions, after a time delay τ. We make a histogram of these displacements, which we average over many different starting times. This yields a PDF of perpendicular displacements. We verified that the PDF is Gaussian, and its width increases linearly with τ, as expected for normal diffusion, as opposed to subdiffusion or superdiffusion.[64,65] We calculate the diffusion coefficient $D_{p\perp}$ as the second moment of the PDF divided by τ. The diffusion coefficients we report in Sec. IV are for a limiting case of large τ.

We verified that our result for $D_{p\perp}$ does not depend on the system size N.

III. INTUITIVE ESTIMATE OF $D_{p\perp}$

We can estimate roughly the expected value of $D_{p\perp}$. First we consider the low regime, which is near equilibrium, so that we make an estimate based on a random-walk argument. The diffusion coefficient will be $D_{p\perp} \approx [\overline{(\delta y)^2} + \overline{(\delta z)^2}]/4\delta t$, where δy and δz are some typical step sizes between collisions, δt is a typical time between collisions. The factor of 4 is chosen for a two-dimensional random walk, since we are interested in only the $\perp$ directions. Estimating that δy and δz are comparable to the Wigner-Seitz radius a, and δt is comparable to $1/\omega_t$, we expect that $D_{p\perp}$ will be roughly $0.25a^2\omega_t$. (In our simulation, we will find the actual value is somewhat smaller than this, and we will find that it depends on the target temperature as well.)

For the high regime, we expect that the diffusion will increase above the near-equilibrium level. To understand why, consider first that as the force is increased, the drift velocity u_p will be larger. Projectiles will thus have a greater momentum in the $\hat{x}$ direction when they undergo a collision with a target particle, so that after the collision the momentum in the $\perp$ direction can be larger than under equilibrium conditions, and this will lead to displacements in the $\perp$ direction that are also larger than for equilibrium. For this reason, we expect $D_{p\perp}$ to increase with u_p in the high regime, and with F and W_p as well. We do not have a model to predict this increase quantitatively; we will instead find it empirically, using our simulation.

IV. RESULTS

A. Projectile's displacement and velocity

Figures 1(a) and 1(b) show typical particle displacements, at two times. In Fig. 1(b), a significant time after a projectile was injected, the projectiles have been scattered significantly in the perpendicular direction, due to collisions mainly with the target particles but also with the neutral gas. This scattering corresponds to the projectile's random walk, or diffusion, in the perpendicular direction. This diffusion is the main topic of this paper.

Example projectile velocities are shown in Figs. 1(c) and 1(d). The earliest time shown is in Fig. 1(c), immediately after injection. This early time represents a transient due to the way our simulation begins; the projectiles have not yet scattered or attained a constant drift speed u_p. Later, after this initial transient, projectiles in Fig. 1(d) have attained a drift speed u_p, and more importantly for the purpose of this paper, their velocities have scattered in the perpendicular direction. In all of our further analysis, we exclude the initial transient period.

B. Mean kinetic energy for projectiles

We characterize the dispersion of the perpendicular velocity by calculating a mean kinetic energy for perpendicular motion

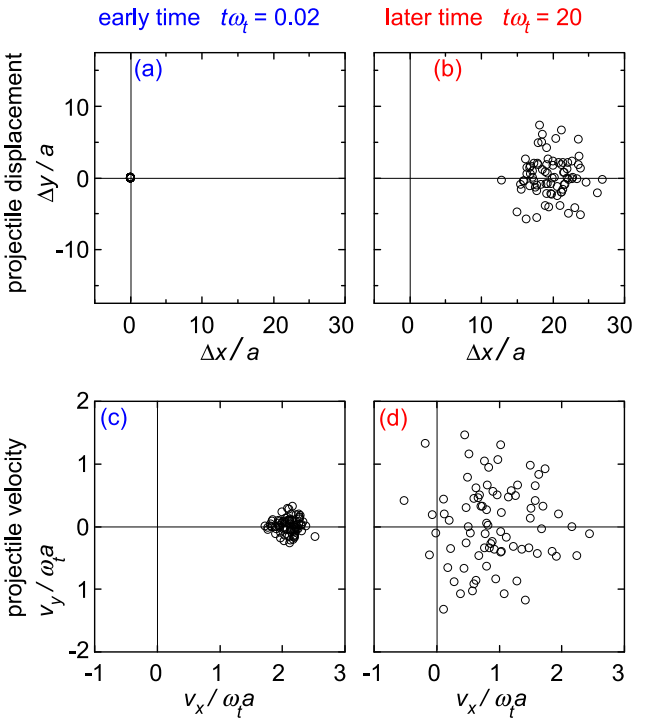

FIG. 1. Diffusion of projectiles due to collisions with charged target particles and neutral gas. (a) A beam of projectiles is injected at a displacement $\Delta x = 0$. (b) The projectiles spread as they drift in the $\hat{x}$ direction. The diffusion of the projectile beam, as seen from the dispersion in (b), is our main focus. Our analysis will be based on random walk displacements in the perpendicular $\hat{y}$ and $\hat{z}$ directions. The velocities of projectiles exhibit an increasing dispersion, starting soon after injection in (c) and increasing later in (d). Data shown here are for $T_t = 2T_m$ and $F = 3\,m_p\omega_t^2 a$, for which the drift speed is $u_p = 0.92\,a\omega_t$.

$$W_p = m_p\overline{(v_y^2 + v_z^2)}/2, \tag{9}$$

which we plot in Figs. 2(a) and 2(b) as a function of F. In preparing these figures from Eq. (9), we averaged over a time interval $5 < t\omega_t < 20$ and over 80 projectiles. Note that W_p describes random motion, which has an average of zero velocity. It does not include the portion of the projectile's kinetic energy due to the drift in the $\|$ direction.

We fit our W_p data to the form

$$\frac{m_t(a\omega_t)^2}{3}\left[\frac{1}{\Gamma_t} + \xi\left(\frac{F}{m_p\omega_t^2 a}\right)^2\right] \tag{10}$$

to characterize the force dependence of W_p. We chose this form by analogy to a theory[66,67] for mobility and diffusion of ion projectiles in neutral gas. That theory predicts an ion energy that is the sum of two terms: a thermal energy k_BT_t and a drift term. The latter is a kinetic energy related to the parallel drift u_p. Our Eq. (10) is written similarly. The terms in the square brackets are dimensionless, so that k_BT_t is replaced by $1/\Gamma_t$. In the drift term, we replace u_p by a factor $\propto F$ since the parallel motion is mobility limited. The form of Eq. (10) provides a smooth transition from the low regime (dominated by the thermal term $1/\Gamma_t$) to the high regime (dominated by the drift term with F). The dimensionless parameter ξ arises physically because of collisional processes such as mobility, and we will allow it to be the only free parameter in the fit.

We find that Eq. (10), shown as smooth curves in Figs. 2(a) and 2(b), fits the data for W_p well for $F < 10\, m_p \omega_t^2 a$. The only free parameter in the fit was ξ, which we determined to be $\xi = 3.6 \times 10^{-4}$. The fit fails, however, for $F > 10\, m_p \omega_t^2 a$, perhaps due to an increasing role of gas friction, as discussed in Sec. IV C.

C. Diffusion and its force dependence

Our chief result is the diffusion coefficient $D_{p\perp}$. We present its values in Figs. 2(c) and 2(d), as a function of force. The diffusion coefficient varies over a range of 0.03 to 2.0 $a^2\omega_t$, for the target temperatures and range of forces that we consider. In physical units, this range corresponds to 0.19 to 12.6 mm^2/s for the PK-4 parameters listed in Sec. II. (This diffusion coefficient for projectiles should not be confused with the diffusion coefficient of the non-drifting target particles, which is 0.0011 or 0.0082 $a^2\omega_t$, for $T_t = 2T_m$ or $10T_m$, respectively.)

We find that the diffusion coefficient $D_{p\perp}$ exhibits different trends in the two force regimes. In the low regime, $D_{p\perp}$ approaches a constant value as the force diminishes. This low-force constant depends on the target temperature; it is $D_{p\perp} = 0.033 \pm 0.006\ a^2\omega_t$ for $T_t = 2T_m$, and $0.21 \pm 0.01\ a^2\omega_t$ for $T_t = 10T_m$. These values for $D_{p\perp}$ are somewhat smaller than our rough estimate in Sec. III, which was based on a simple random-walk argument. Moreover, $D_{p\perp}$ also depends on target temperature, which was not anticipated by our rough estimate.

We can empirically characterize the data for $D_{p\perp}$ in both regimes by fitting them to a single function of force and target temperature. In Figs. 2(c) and 2(d), we find that the data are fit well by an expression

$$a^2\omega_t \left\{ A \left[\frac{1}{\Gamma_t} + \beta \left(\frac{F}{m_p \omega_t^2 a} \right)^2 \right] \right\}^C . \tag{11}$$

We chose the form of Eq. (11) in analogy to Eq. (10), but with an exponent C. This exponent is required at high forces because we find that the power law dependences of $D_{p\perp}$ and W_p with respect to F are not the same. The temperature dependence is reflected by the term with $1/\Gamma_t$ and, to a lesser extent, the exponent C. The free parameters, for the best fit shown as smooth curves, are $A = 2.3 \pm 0.1$ and $\beta = 0.0031 \pm 0.0002$. The third free parameter, C, varies weakly with the target temperature, with $C = 0.73 \pm 0.02$ and 0.49 ± 0.09 for $T_t = 2T_m$ and $10T_m$, respectively.

The power law dependence of $D_{p\perp}$ in the high regime depends on target temperature. This is different from the behavior of W_p in the high regime, which had the same quadratic scaling in both regimes. Based on our fit, we find that

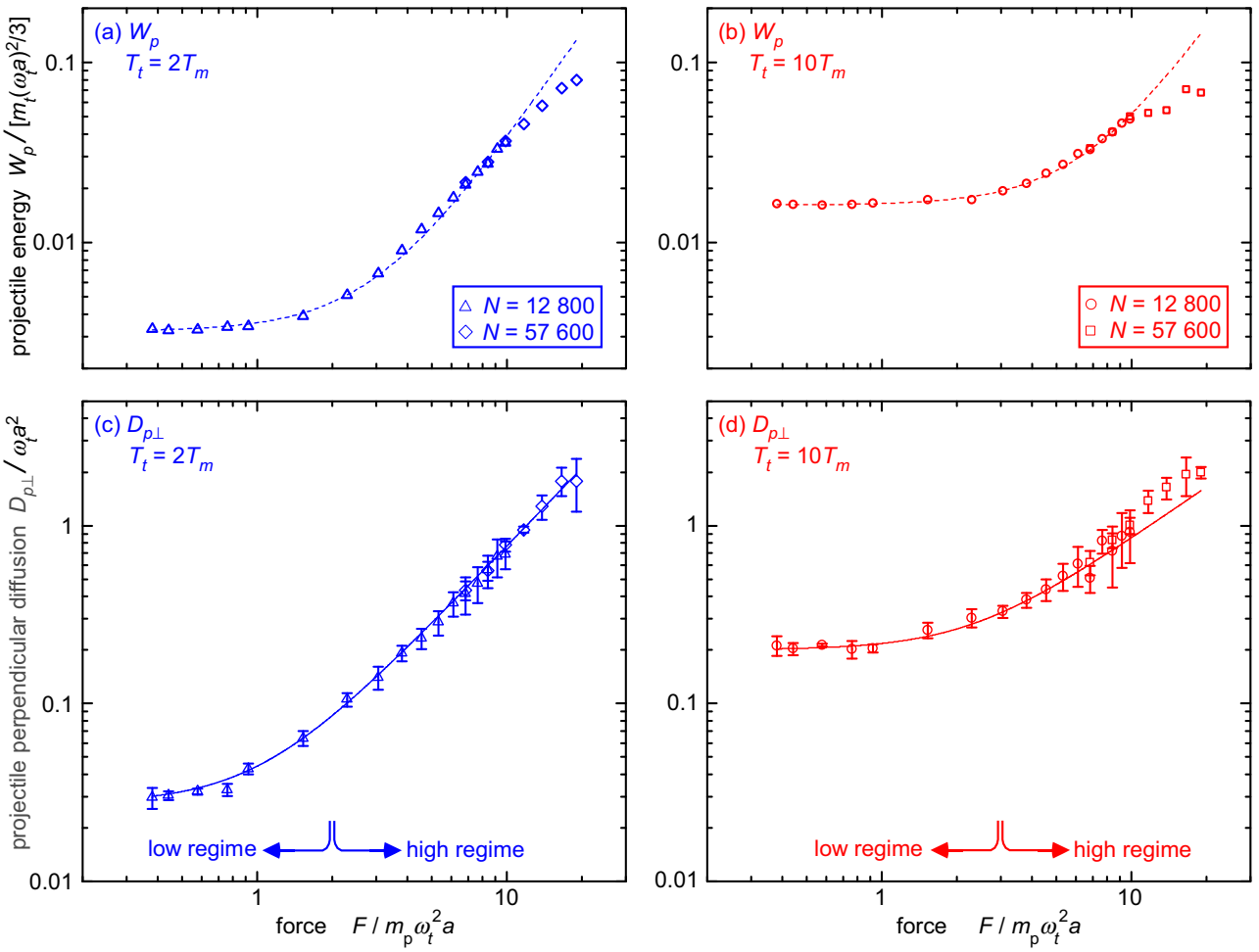

FIG. 2. Mean kinetic energy W_p dependence on F for: (a) $T_t = 2T_m$ and (b) $T_t = 10T_m$. The dashed curves are fits to Eq. (10). The perpendicular diffusion coefficient $D_{p\perp}$, which is our main result, is shown for (c) $T_t = 2T_m$ and (d) $T_t = 10T_m$. The solid curves are fits to Eq. (11). In the high regime (large F), $D_{p\perp} \propto F^{1.5}$ for $T_t = 2T_m$ and $D_{p\perp} \propto F^{1.0}$ for $T_t = 10T_m$. The transition between the low and high regimes, as was identified in Ref. 58, is indicated by arrows.

the power law scaling is $D_{p\perp} \propto F^{1.46\pm0.04}$ for the low temperature $T_t = 2T_m$, but $D_{p\perp} \propto F^{0.98\pm0.18}$ for the high temperature $T_t = 10T_m$.

We expect that our fitting expressions, Eq. (10) for W_p and Eq. (11) for $D_{p\perp}$, will not apply in a third regime[58] at higher forces. In this third regime, we expect neutral gas will play a larger role. However, neutral gas is not accounted for in Eqs. (10) and (11). We can explain conceptually how the scaling of W_p and $D_{p\perp}$ will change in this third regime. Consider that the drift velocity u_p is the source of the enhanced scattering in the high regime. This scattering will take a different character when it is determined not just by target particles, but gas as well. Since W_p and $D_{p\perp}$ are due to the scattering, the different scattering character in the third regime could lead to a different scaling. There may be a hint of this third regime in Figs. 2(a) and 2(b) for $F > 10\, m_p\omega_t^2 a$, but we have not explored this third regime in detail.

D. Energy dependence of diffusion

An obvious question to ask about diffusion, in equilibrium systems, is how the diffusion coefficient depends on temperature. In the case with a dilute beam, the projectiles do not have a temperature, because they are driven by a force and therefore they are not in thermal equilibrium. We can, however, report our diffusion coefficient as a function of the mean kinetic energy W_p for the projectile's random motion. We do this by replotting the data in Fig. 2, eliminating F.

The results for the energy dependence of $D_{p\perp}$ are shown in Fig. 3. We find that the diffusion coefficient $D_{p\perp}$ increases monotonically with the mean kinetic energy W_p. This increase is nearly linear for high energies. For lower energies, the dependence is nearly exponential.

For high energies, the normalized data points for the two target temperatures overlap in Fig. 3. This overlap suggests that $D_{p\perp}$ vs W_p is self similar with respect to a change in target temperature. A comparable similarity is not seen in the force dependence, Figs. 2(c) and 2(d) for $D_{p\perp}$ vs F.

For the high energies, where the results are the same for both target temperatures, we find that our data in Fig. 3 scale as $D_{p\perp} \propto W_p^{1.0}$. Fitting to this form, we find an empirical linear relationship $D_{p\perp} = 60W_p/m_t\omega_t$. This fit is shown as a straight line in Fig. 3.

For the lowest energies in Fig. 3, the curve for $D_{p\perp}$ vs W_p rolls off, and the linear relationship above fails. This rolloff occurs at $W_p < 3.5k_BT_t$ for $T_t = 2\,T_m$ and $W_p < 1.5k_BT_t$ for $T_t = 10T_m$. Instead of a linear dependence, the data in this rolloff exhibit a dependence that is nearly, but not exactly, exponential, $D_{p\perp} \propto e^{-E_a/W_p}$. This exponential dependence resembles the Arrhenius dependence of diffusion for impurity atoms in a solid, where an atom must surmount a potential barrier E_a in order to diffuse.[68] In our physical system, the energy E_a might correspond to some physical quantity other than just a *potential* barrier, because we found that E_a depends on the target temperature.[69]

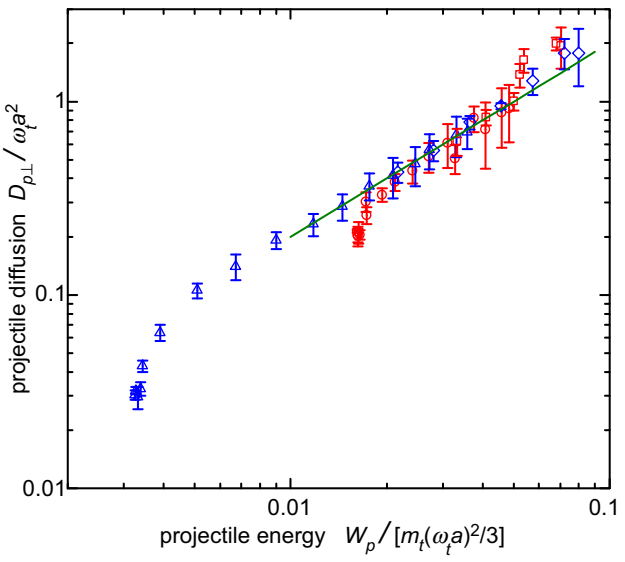

FIG. 3. Energy dependence of the diffusion coefficient $D_{p\perp}$. Note that the data points for both target temperatures fall on a common curve for $W_p/[m_t(\omega_t a)^2/3] > 0.02$. The straight line is $D_{p\perp} = 60W_p/m_t\omega_t$, which is a linear fit for high energies. The symbols are as in the legends in Fig. 2. We combined the data for $T_t = 2T_m$ to obtain the triangles and diamonds, and the data for $10T_m$ to obtain the circles and squares.

V. SUMMARY

In summary, we investigated the perpendicular diffusion of a charged projectile drifting through a strongly coupled dusty plasma. Such a drift can occur due to a net force that acts only on projectiles but not on target particles of a different size. In a dusty plasma, a net force can be nonzero due to unbalanced electric and ion drag forces.

The diffusion coefficient $D_{p\perp}$ was determined from the simulation data. We found values ranging from 0.03 to 2.0 $a^2\omega_t$, depending on the force and target temperature.

We found that the force affects a projectile's diffusion differently in two regimes, for low and high forces. In the low force regime, the diffusion coefficient approaches a constant, but in the high regime, $D_{p\perp}$ increases with the force with a power law scaling that depends on target temperature. The computed value in the low regime is somewhat smaller than our rough estimate $0.25a^2\omega_t$ based on a random-walk argument, and it also depends on the target temperature.

We also investigated the energy dependence of the diffusion coefficient. In terms of a mean kinetic energy W_p, we empirically found that $D_{p\perp} = 60W_p/m_t\omega_t$, for high energies. This same linear function applies for both target temperatures that we simulate. For low energies, however, $D_{p\perp}$ varies nearly exponentially with W_p, not linearly.

We anticipate that the diffusion process studied here can be observed experimentally. Doing this in a dusty plasma would require tracking the projectile particles for a sufficiently long time to evaluate the diffusion coefficient. The feasibility of this measurement was considered in Ref. 59.

ACKNOWLEDGMENTS

This work was supported by NASA and NSF. We thank W. D. S. Ruhunusiri and F. Skiff for helpful discussions.

[1]P. K. Shukla and A. A. Mamun, *Introduction to Dusty Plasma Physics* (Institute of Physics, Bristol, 2002).
[2]O. Ishihara, J. Phys. D: Appl. Phys. **40**, R121 (2007).
[3]A. Melzer and J. Goree, in *Low Temperature Plasmas: Fundamentals, Technologies and Techniques*, 2nd ed., edited by R. Hippler, H. Kersten, M. Schmidt, and K. H. Schoenbach (Wiley-VCH, Weinheim, 2008), p. 129.
[4]G. E. Morfill and A. V. Ivlev, Rev. Mod. Phys. **81**, 1353 (2009).
[5]V. E. Fortov and G. E. Morfill, *Complex and Dusty Plasma: From Laboratory to Space, Series in Plasma Physics* (CRC Press, New York, 2009).
[6]M. Bonitz, C. Henning, and D. Block, Rep. Prog. Phys. **73**, 066501 (2010).
[7]A. Piel, *Plasma Physics* (Springer, Heidelberg, 2010).
[8]H. Thomas, G. E. Morfill, V. Demmel, J. Goree, B. Feuerbacher, and D. Mohlmann, Phys. Rev. Lett. **73**, 652 (1994).
[9]J. H. Chu and I. Lin, Phys. Rev. Lett. **72**, 4009 (1994).
[10]A. Melzer, A. Homann, and A. Piel, Phys. Rev. E **53**, 2757 (1996).
[11]B. Liu, J. Goree, V. Nosenko, and L. Boufendi, Phys. Plasmas **10**, 9 (2003).
[12]Y. Feng, J. Goree, and B. Liu, Rev. Sci. Instrum. **78**, 053704 (2007).
[13]T. M. Flanagan and J. Goree, Phys. Rev. E **80**, 046402 (2009).
[14]S. Ichimaru, Rev. Mod. Phys. **54**, 1017 (1982).
[15]G. E. Morfill, H. M. Thomas, U. Konopka, H. Rothermel, M. Zuzic, A. Ivlev, and J. Goree, Phys. Rev. Lett. **83**, 1598 (1999).
[16]A. P. Nefedov, G. E. Morfill, V. E. Fortov, H. M. Thomas, H. Rothermel, T. Hagl, A. V. Ivlev, M. Zuzic, B. A. Klumov, A. M. Lipaev, V. I. Molotkov, O. F. Petrov, Y. P. Gidzenko, S. K. Krikalev, W. Shepherd, A. I. Ivanov, M. Roth, H. Binnenbruck, J. A. Goree, and Y. P. Semenov, New J. Phys. **5**, 33 (2003).
[17]H. M. Thomas, G. E. Morfill, V. E. Fortov, A. V. Ivlev, V. I. Molotkov, A. M. Lipaev, T. Hagl, H. Rothermel, S. A. Khrapak, R. K. Suetterlin, M. Zuzic, O. F. Petrov, V. I. Tokarev, and S. K. Krikalev, New J. Phys. **10**, 033036 (2008).
[18]A. Piel, M. Klindworth, O. Arp, A. Melzer, and M. Wolter, Phys. Rev. Lett. **97**, 205009 (2006).
[19]M. H. Thoma, H. Hofner, M. Kretschmer, S. Ratynskaia, G. E. Morfill, A. Usachev, A. Zobnin, O. Petrov, and V. Fortov, Microgravity Sci. Technol. **18**, 47 (2006).
[20]W. T. Juan and I. Lin, Phys. Rev. Lett. **80**, 3073 (1998).
[21]Y. K. Khodataev, S. A. Khrapak, A. P. Nefedov, and O. F. Petrov, Phys. Rev. E **57**, 7086 (1998).
[22]O. S. Vaulina, A. P. Nefedov, O. F. Petrov, and V. E. Fortov, Phys. Rev. Lett. **88**, 035001 (2002).
[23]V. E. Fortov, Plasma Phys. Controlled Fusion **46**, B359 (2004).
[24]O. F. Petrov, O. S. Vaulina, V. E. Fortov, V. I. Molotkov, A. M. Lipaev, A. V. Chernyshev, A. V. Gavrikov, I. N. Shakhova, G. E. Morfill, H. Thomas, S. A. Khrapak, Y. P. Semenov, A. I. Ivanov, A. Y. Kaleri, S. Krikalev, S. V. Zaletin, and Y. Gidzenko, Microgravity Sci. Technol. **16**, 311 (2005).
[25]S. Ratynskaia, K. Rypdal, C. Knapek, S. Khrapak, A. V. Milovanov, A. Ivlev, J. J. Rasmussen, and G. E. Morfill, Phys. Rev. Lett. **96**, 105010 (2006).
[26]S. Nunomura, D. Samsonov, S. Zhdanov, and G. Morfill, Phys. Rev. Lett. **96**, 015003 (2006).
[27]B. Liu and J. Goree, Phys. Rev. Lett. **100**, 055003 (2008).
[28]B. Liu, J. Goree, and Y. Feng, Phys. Rev. E **78**, 046403 (2008).
[29]C. W. Io and I. Lin, Phys. Rev. E **85**, 026407 (2012).
[30]T. S. Ramazanov, A. N. Jumabekov, S. A. Orazbayev, M. K. Dosbolayev, and M. N. Jumagulov, Phys. Plasmas **19**, 023706 (2012).
[31]A. Schella, M. Mulsow, A. Melzer, J. Schablinski, and D. Block, Phys. Rev. E **87**, 063102 (2013).
[32]H. Ohta and S. Hamaguchi, Phys. Plasmas **7**, 4506 (2000).
[33]O. Vaulina and S. V. Vladimirov, Phys. Plasmas **9**, 835 (2002).
[34]O. S. Vaulina, S. Khrapak, and G. Morfill, Phys. Rev. E **66**, 016404 (2002).
[35]O. S. Vaulina, S. V. Vladimirov, O. F. Petrov, and V. E. Fortov, Phys. Plasmas **11**, 3234 (2004).
[36]O. S. Vaulina, I. E. Drangevski, X. G. Adamovich, O. F. Petrov, and V. E. Fortov, Phys. Rev. Lett. **97**, 195001 (2006).
[37]B. Liu, J. Goree, and O. S. Vaulina, Phys. Rev. Lett. **96**, 015005 (2006).
[38]B. Liu and J. Goree, Phys. Rev. E **75**, 016405 (2007).
[39]T. Ott, M. Bonitz, Z. Donko, and P. Hartmann, Phys. Rev. E **78**, 026409 (2008).
[40]Z. Donko, J. Goree, P. Hartmann, and B. Liu, Phys. Rev. E **79**, 026401 (2009).
[41]Z. Donko, J. Phys. A: Math. Theor. **42**, 214029 (2009).
[42]T. Ott and M. Bonitz, Phys. Rev. Lett. **103**, 195001 (2009).
[43]T. Ott and M. Bonitz, Contrib. Plasma Phys. **49**, 760 (2009).
[44]L. J. Hou, A. Piel, and P. K. Shukla, Phys. Rev. Lett. **102**, 085002 (2009).
[45]S. Ratynskaia, G. Regnoli, K. Rypdal, B. Klumov, and G. Morfill, Phys. Rev. E **80**, 046404 (2009).
[46]O. S. Vaulina, Y. V. Khrustalyov, O. F. Petrov, and V. E. Fortov, EPL **89**, 35001 (2010).
[47]S. Ratynskaia, G. Regnoli, B. Klumov, and K. Rypdal, Phys. Plasmas **17**, 034502 (2010).
[48]Y. Feng, J. Goree, and B. Liu, Phys. Rev. E **82**, 036403 (2010).
[49]T. Ott and M. Bonitz, Phys. Rev. Lett. **107**, 135003 (2011).
[50]S. A. Khrapak, O. S. Vaulina, and G. E. Morfill, Phys. Plasmas **19**, 034503 (2012).
[51]K. N. Dzhumagulova, T. S. Ramazanov, and R. U. Masheeva, Phys. Plasmas **20**, 113702 (2013).
[52]A. Shahzad, M. G. He, and K. He, Phys. Scr. **87**, 035501 (2013).
[53]H. Charan, R. Ganesh, and A. Joy, Phys. Plasmas **21**, 043702 (2014).
[54]J. Goree, G. E. Morfill, V. N. Tsytovich, and S. V. Vladimirov, Phys. Rev. E **59**, 7055 (1999).
[55]K. R. Sütterlin, A. Wysocki, A. V. Ivlev, C. Rath, H. M. Thomas, M. Rubin-Zuzic, W. J. Goedheer, V. E. Fortov, A. M. Lipaev, V. I. Molotkov, O. F. Petrov, G. E. Morfill, and H. Löwen, Phys. Rev. Lett. **102**, 085003 (2009).
[56]K. R. Sütterlin, H. M. Thomas, A. V. Ivlev, G. E. Morfill, V. E. Fortov, A. M. Lipaev, V. I. Molotkov, O. F. Petrov, A. Wysocki, and H. Löwen, IEEE Trans. Plasma Sci. **38**, 861 (2010).
[57]M. A. Fink, M. H. Thoma, and G. E. Morfill, Microgravity Sci. Technol. **23**, 169 (2011).
[58]B. Liu and J. Goree, Phys. Rev. E **89**, 043107 (2014).
[59]J. Goree, B. Liu, and Y. Feng, Plasma Phys. Controlled Fusion **55**, 124004 (2013).
[60]These friction constants were calculated using a leading coefficient of 1.26 in the Epstein drag formula.[11]
[61]S. A. Khrapak, S. Ratynskaia, A. V. Zobnin, A. D. Usachev, V. V. Yaroshenko, M. H. Thoma, M. Kretschmer, H. Höfner, G. Morfill, O. F. Petrov, and V. E. Fortov, Phys. Rev. E **72**, 016406 (2005).
[62]V. Fortov, G. Morfill, O. Petrov, M. Thoma, A. Usachev, H. Hoefner, A. Zobnin, M. Kretschmer, S. Ratynskaia, M. Fink, K. Tarantik, Y. Gerasimov, and V. Esenkov, Plasma Phys. Controlled Fusion **47**, B537 (2005).
[63]S. Hamaguchi, R. T. Farouki, and D. H. E. Dubin, Phys. Rev. E **56**, 4671 (1997).
[64]T. H. Solomon, E. R. Weeks, and H. L. Swinney, Phys. Rev. Lett. **71**, 3975 (1993).
[65]S. Ratynskaia, C. Knapek, K. Rypdal, S. Khrapak, and G. Morfill, Phys. Plasmas **12**, 022302 (2005).
[66]E. A. Mason and E. W. McDaniel, *Transport Properties of Ions in Gases* (John Wiley & Sons, New York, 1988).
[67]G. H. Wannier, Phys. Rev. **87**, 795 (1952).
[68]C. Kittel, *Introduction to Solid State Physics* (John Wiley & Sons, New York, 1976).
[69]We found that E_a is of order $0.0031\, m_t \omega_t^2 a^2$ for $T_t = 2\mathrm{Tm}$ and $0.013\, m_t \omega_t^2 a^2$ for $10T_m$. These results are from fitting to an exponential. The fit was reasonably good with $R^2 = 0.9$, and this fit quality is reflected in our observation that the dependence of D_p on W_p is *nearly* exponential, at low energies.